Programmed *in vivo* excision of prophage Φ13 is an essential timing device for the *Staphylococcus aureus* infectious process

Olivier Poupel,[1] Gérald Kenanian,[1] Lhousseine Touqui,[2] Charlotte Abrial,[2] Grégory Jouvion,[3,4] Tarek Msadek[1,6*], Sarah Dubrac[1,5,6*]

[1] Institut Pasteur, Université Paris Cité, CNRS UMR2001, Department of Microbiology, Biology of Gram-Positive Pathogens Unit, F-75015 Paris, France

[2] Institut Pasteur, Université Paris Cité, Department of Global Health, Cystic Fibrosis and Bronchial Diseases Unit, F-75015 Paris, France.

[3] Institut Pasteur, Université Paris Cité, Department of Infection and Epidemiology, Experimental Neuropathology Unit, F-75015 Paris, France

[4]Present address: Ecole Nationale Vétérinaire d'Alfort, Veterinary Histology and Pathology Unit, Maisons-Alfort, France

[5]Present address: Institut Pasteur, Université Paris Cité, CNRS UMR6047, Department of Microbiology, Stress Adaptation and Metabolism in Enterobacteria Unit, F-75015 Paris, France

[6]These authors jointly supervised this work : Tarek Msadek, Sarah Dubrac.

*Address correspondence to Tarek Msadek, tmsadek@pasteur.fr, or Sarah Dubrac sarah.dubrac@pasteur.fr

ABSTRACT Mobile genetic elements play an essential part in the infectious process of major pathogens, yet the role of prophage dynamics in *Staphylococcus aureus* remains poorly understood. Here we studied the impact of the Φ13 *hlb*-converting prophage, whose integration inactivates the *hlb* β-toxin gene, on staphylococcal pathogenesis. We showed that prophage Φ13 is lost in approximately half the bacterial population during the course of infection. Inactivation of the Φ13 *int* recombinase gene, essential for insertion/excision, locked the prophage in the bacterial chromosome, leading to a significant loss of virulence in a murine systemic infection model. In contrast, the non-lysogen strain (ΔΦ13), where the *hlb* beta-hemolysin gene is reconstituted, displayed strongly increased virulence. Accordingly, histopathological analyses revealed more severe nephritis in mice infected with bacteria lacking prophage Φ13 (ΔΦ13), in contrast to infection with the parental strain and particularly with the Δ*int* mutant, which led to less severe renal lesions. Cytokine induction in a human neutrophil model showed significantly increased IL-6 expression following infection with the beta-hemolysin producing strain (ΔΦ13). Our results indicate that programmed *in vivo* excision of the Φ13 prophage is essential for progression of the *Staphylococcus aureus* infectious process, since early excision rapidly kills the host whereas the absence of excision significantly lowers staphylococcal virulence.

IMPORTANCE This study highlights prophage Φ13 excision as a critical factor in *S. aureus* pathogenesis, influencing infection outcomes by balancing rapid host killing with reduced bacterial virulence. This mechanism may represent a bet-hedging strategy in genetic regulation, resulting in a mixed bacterial population capable of rapidly switching between two processes: bacterial colonization and host damage. Unraveling this dynamic opens new possibilities for developing targeted therapies to disrupt or modulate prophage activity, offering a novel approach to mitigating *S. aureus* infections.

55 **INTRODUCTION**

56 *Staphylococcus aureus*, a major human pathogen, causes severe invasive infectious
57 diseases targeting every type of organ, such as pneumonia, endocarditis, osteomyelitis
58 or septicemia. Yet it is also a commensal, asymptomatically colonizing up to 30% of
59 the human population, with the transition between the two lifestyles poorly
60 understood (1). Mobile genetic elements make up approximately 20% of its genome,
61 leading to variations in gene combinations that can strongly influence *S. aureus*
62 virulence (2). Among these, temperate bacteriophages play an important role in
63 genetic variability. Φ13, a member of the Sa3int Siphoviridae *S. aureus* bacteriophage
64 family, is responsible for a dual phenotypic conversion (3, 4) and is by far the most
65 widespread among human clinical isolates (5). Its chromosomal attachment site (*attB*)
66 lies within the coding sequence of the hemolysin B gene, *hlb*, encoding the neutral
67 sphingomyelinase C β-toxin, such that it acts as a phage regulatory switch (6). Φ13
68 lysogeny leads to disruption of *hlb* and loss of β-hemolytic activity, with excision
69 reconstituting an intact *hlb* gene (5, 7).

70 Phage Φ13 also carries the *iec* immune evasion cluster including several genes
71 involved in escape from the host innate immune response: *scn*, *chp* and *sak* (8, 9).
72 Natural mobility has been shown for the Φ13-related ΦSa3mw phage in strain MW2
73 during murine skin colonization and rabbit invasive infection (10, 11).

74 We studied the effect of phage Φ13 on *S. aureus* virulence during systemic
75 infection. We show that timing of Φ13 prophage excision is essential for pathogenesis,
76 with early β-hemolysin production leading to a strong increase in virulence and
77 elevated levels of the pro-inflammatory cytokine IL-6.
78

79 **RESULTS**

80

81 **Mobility dynamics of *Staphylococcus aureus* prophages**

82

83 *S. aureus* strain HG001, a derivative of NCTC 8325 (12), carries prophages Φ11, Φ12
84 and Φ13 (7, 13). Specific oligonucleotide primer pairs were designed to detect the
85 presence or absence of each prophage (Supplementary Table 2 and Supplementary Fig.
86 1A). Using chromosomal DNA from a closely related strain cured of all phages,
87 SH1000, an amplicon corresponding to the native bacterial locus without Φ13
88 (oligonucleotide pair OMA7/OMA9, hybridizing on either side of the *attB* site) was
89 detected, but no amplification occurred with oligonucleotides specific for Φ13
90 insertion (OMA7/OMA8) (Supplementary Fig. 1B). With the HG001 Φ13 lysogen
91 strain, both types of amplicon were generated by PCR, suggesting spontaneous Φ13
92 excision within the bacterial population (Supplementary Fig. 1B). We quantified
93 relative prophage levels within the bacterial population by qRT-PCR during growth
94 under optimal laboratory conditions (TSB at 37°C with aeration). Our results indicate
95 that prophage Φ11 is highly mobile with approximately 10% of cells lacking the phage
96 whereas Φ12 was much more stable with less than 0.01% of non-lysogen cells (Fig. 1A).
97 Interestingly, the Φ13 prophage was lost in about 0.5% of the population under these
98 growth conditions (Fig. 1A).

99

100 **Excision of prophage Φ13 is increased *in vivo***

101

102 As shown above, prophage Φ13 is spontaneously excised during growth in laboratory
103 conditions. Since this phage carries genes encoding the SAK staphylokinase virulence
104 factor, as well as SCIN and CHIP, involved in escape from the innate immune response
105 (14), we examined Φ13 excision frequency during the infectious process.

106 We generated a strain carrying the *aad*(9) spectinomycin resistance gene inserted
107 within the Φ13 genome (see Materials and Methods, and Supplementary Table 1 strain
108 ST1387). Four days following sub-lethal (2 x 10^7 c.f.u.) intravenous inoculation with *S.*
109 *aureus* strain ST1387, mice were sacrificed and kidneys collected for c.f.u. counts. Out
110 of 25 harvested kidneys, 18 were colonized by a mixed bacterial population with
111 respect to Φ13 lysogeny (Fig.1B). In some mice a single kidney was colonized with a

112 mixed population with the other only by Φ13 lysogens, suggesting that loss of Φ13 is
113 a *post facto* event to kidney colonization. The average loss of Φ13 was around 50% in
114 the 18 kidneys colonized with a mixed bacterial population (Fig. 1C), a significant
115 increase over the spontaneous excision rate of 0.5% observed during growth *in vitro*.
116 These results suggest that Φ13 excision can be induced and/or the non-lysogen
117 population favored during the infectious process under conditions such as those
118 encountered during kidney colonization.
119
120 **Excision of prophage Φ13 is essential for the *S. aureus* infectious process**
121
122 Increased prophage Φ13 excision during infection suggests it may impact virulence.
123 The Φ13 SAOUHSC-*02293* gene, referred to henceforth as *int*, encodes a protein highly
124 similar to tyrosine recombinase integrases such as Int of phage lambda (13, 15). We
125 deleted the entire coding sequence of the Φ13 *int* gene in *S. aureus* strain HG001 to lock
126 the prophage within the bacterial chromosome. We also constructed a strain where the
127 entire Φ13 genome is deleted, restoring an intact and functional *hlb* gene (see Materials
128 and Methods). These mutations had no effect on bacterial growth *in vitro*
129 (Supplementary Fig. 2). β-hemolytic activity following Φ13 excision was detected on
130 sheep blood agar plates as a distal cold-inducible halo of partial hemolysis (indicated
131 by the white arrow in Fig. 2A).
132 As shown in Fig. 2B, the frequency of Φ13 excision in the Δ*int* mutant is lowered
133 more than 1000-fold as compared to that of the wild type strain (0.6%), confirming the
134 essential role of Int in Φ13 excision. Full complementation of the Δ*int* mutant was
135 obtained by expressing the *int* gene from the Pprot constitutive promoter in the
136 pMK4Pprot-*int* plasmid (Fig. 2B).
137 We next examined the effect on *S. aureus* virulence of either the absence of
138 prophage Φ13 (HG001ΔΦ13 strain, intact *hlb* gene) or the lack of Φ13 excision
139 (HG001Δ*int* strain, *hlb* gene disrupted). As shown in Fig. 3A, using a systemic model
140 of murine infection (5 X 10^7 c.f.u. intravenous injection), the absence of Φ13 with a
141 resulting intact *hlb* gene led to acute virulence with the rapid death of infected animals
142 (50% mortality 24 h post-infection for the ΔΦ13 strain vs. six days for the wild type
143 strain), and more than 90% mortality at the end of the assay (ten days post-infection).
144 Conversely, when Φ13 excision is abolished (Δ*int* strain), *S. aureus* virulence is strongly

145 reduced compared to the wild type strain (31% mortality at the end of the assay, *vs*
146 63%). These results indicate that Φ13 excision and its timing are crucial parameters for
147 the *S. aureus* infectious process.
148
149 **Φ13 dynamics are involved in organ damage during infection**
150
151 To understand the effect of Φ13 dynamics on *S. aureus* virulence, we measured
152 bacterial colonization, and evaluated the kidney lesions of infected mice by
153 histopathological analysis. Mice were inoculated intravenously with sub-lethal
154 concentrations of *S. aureus* cells (approximately 2 X 10^7 c.f.u.). At six days post-infection,
155 mice were sacrificed and one kidney was fixed for histopathological analysis and the
156 other homogenized for c.f.u. counts. Kidney bacterial loads for the parental HG001
157 strain and the HG001ΔΦ13 and HG001Δ*int* mutants were not significantly different
158 (approximately 5 X 10^7 c.f.u. per kidney; Supplementary Fig. 3). However,
159 histopathological analysis revealed nephritis (very probably embolic nephritis) with
160 significantly varying degrees of severity between mice infected with the parental
161 HG001 strain or the ΔΦ13 and Δ*int* mutants. At six days post-infection, mice inoculated
162 with the wild type strain generally displayed mild to moderate nephritis (5/6 mice) or
163 multifocal inflammatory infiltrates (macrophages and other mononucleated cells) in
164 the renal cortex (1/6 mouse) (Fig. 3B1 and 3B2). In contrast, the ΔΦ13 strain leads to
165 more severe nephritis (5/6 mice), with neutrophilic inflammation forming multifocal
166 abscesses, extension to tubules and interstitium, and ischemic necrosis of the papillae
167 (Fig. 3B3 and 3B4). Mice infected with the Δ*int* strain displayed less severe lesions, with
168 mononuclear cell infiltrates mostly in the cortex (4/6 mice) or mild to moderate (1/6
169 mouse) or marked (1/6 mouse) nephritis (Fig. 3B5 and 3B6).
170 These results show that Φ13 dynamics and correlated β-hemolysin production
171 are not essential for host colonization but instead are key factors in host organ damage
172 during infection.
173
174 **Φ13 excision triggers host inflammatory response in infected THP-1 cells**
175
176 Given the major impact of Φ13 excision on virulence and inflammation, we tested its
177 effect on induction of the cellular inflammatory response using human monocytic
178 THP-1 cells. We compared the bacterial internalization capacity of THP-1 cells, the

179 intracellular viability of bacterial cells and the induction of inflammatory markers
180 following infection with the parental HG001 strain and the ΔΦ13 and Δ*int* mutants.
181 THP-1 differentiated macrophages were very efficient for *S. aureus* phagocytosis
182 regardless of prophage content, with nearly 100% of bacteria internalized with a MOI
183 (Multiplicity of Infection) of 10 after 2 hours (Supplementary Fig. 4A). Intracellular
184 survival was not significantly different for the three strains with approximately 10%
185 survival after 24 h post infection and less than 5% after 48 h (Supplementary Fig. 4B).
186 To measure induction of the inflammatory response, duplicate aliquots of infected
187 THP-1 cells were frozen 24 h post-infection, treated to recover cellular RNA and
188 induction of inflammatory cytokine genes measured by qRT-PCR. We measured
189 induction of three pro-inflammatory cytokines previously shown to be induced by
190 *S. aureus* infection, TNFα, IL-1β and IL-6 (16). Although there was no significant
191 difference in induction levels of TNFα and Pro-IL-1β for the three strains, IL-6 gene
192 expression was strongly increased when THP-1 cells were infected with the ΔΦ13
193 strain as compared to the HG001 strain and the Δ*int* mutant (Fig. 4). Thus, lysogeny
194 by Φ13 and the concomitant loss of β-hemolytic activity appear to down-regulate the
195 inflammatory response through lower induction of the pro-inflammatory cytokine IL-
196 6.
197
198 **Impact of *hlb* on *S. aureus* virulence**
199
200 Taken together the results shown above suggest a major role of β-hemolysin
201 production in the increased virulence of the ΔΦ13 strain. To test this hypothesis, we
202 compared the virulence of the ΔΦ13 strain, which produces β-hemolysin, with the
203 virulence of the ΔΦ13Δ*hlb* strain in which the *hlb* gene has also been deleted. As shown
204 in Fig. 5A, 44% of mice infected by the ΔΦ13Δ*hlb* strain survived at nine days post-
205 infection, whereas survival of mice infected by the strain producing β-hemolysin
206 (ΔΦ13) was only 14%, indicating that it is the major factor responsible for the effect of
207 Φ13 excision on *S. aureus* virulence. To test the contribution of Φ13 in virulence, we
208 constructed a strain where both Φ13 and an intact *hlb* gene are present (Δ*int hlb*
209 complemented strain; see Materials and Methods, and Supplementary Table 1). As
210 shown in Fig. 5B, mouse mortality caused by the ΔΦ13 strain producing β-hemolysin
211 but lacking the Φ13 prophage was essentially the same as that following infection by

212 the Δ*int hlb* complemented strain (with both the Φ13 prophage and a functional *hlb*
213 gene). This result confirms the major role of Φ13 dynamics in *S. aureus* virulence by
214 controlling timing of β-hemolysin production during the infectious process.
215

216 **DISCUSSION**

217 *Staphylococcus aureus* is a highly successful human pathogen with a sophisticated
218 arsenal of virulence factors whose production is tightly controlled by multiple
219 regulatory networks, such as two-component systems (17). Further fine-tuning is
220 provided by mobile genetic elements such as pathogenicity islands (SaPI), plasmids,
221 transposons, staphylococcal cassette chromosomes (SCC) and bacteriophages
222 conferring additional virulence factors or antibiotic resistance genes (18). Prophages
223 are widely distributed amongst *S. aureus* strains. Among these, the Φ13 *S. aureus*
224 prophage is inserted within the *hlb* gene encoding β-hemolysin and carries at least
225 three genes involved in host interactions and escape from the immune response,
226 known as the immune evasion cluster (IEC): *sak*, encoding staphylokinase, involved in
227 converting host plasminogen to active plasmin, *scn*, encoding a staphylococcal
228 complement inhibitor, and *chp*, encoding a neutrophil and monocyte chemotaxis
229 inhibitory protein (8). The Φ13 *hlb*-converting prophage family is present in
230 approximately 90% of *S. aureus* clinical isolates (8).

231 β-hemolysin is a sphingomyelinase that can lyse proliferating human
232 lymphocytes, contributing to the host immune evasion (19). Independently of its pore
233 forming activity, β -hemolysin has a biofilm ligase effect by forming a nucleoprotein
234 matrix both in vitro and during infectious endocarditis (20, 21). It has also been shown
235 that Hlb favors mouse skin colonization (11). We noted that *S. aureus* cells isolated
236 from infected mice frequently displayed β-hemolytic activity due to *in vivo* excision of
237 the Φ13 prophage. This prompted us to examine the effect of phage mobility on host
238 pathogen interactions. Our results indicate that mobility of this prophage is required
239 for full virulence of *S. aureus* as part of the time-course of the infectious process. We
240 identified and inactivated the potential integrase gene of this prophage, effectively
241 locking the prophage within the *S. aureus* genome by preventing its excision, and
242 showed that this leads to strongly decreased virulence, with 70% of the mice still
243 surviving after 10 days. Conversely, a strain lacking the Φ13 prophage exhibited
244 greater virulence than the wild type strain, particularly evident in the rapid mortality
245 of infected mice, with 50% succumbing within the first day of infection, compared to
246 six days for the wild-type strain. These Φ13-associated virulence traits are not
247 correlated to differences in the strain's ability to colonize the host, as bacterial loads in
248 the infected kidneys were similar regardless of the strain's lysogenic status. However,

249 kidney damage following infection was strongly associated with the presence of Φ13,
250 showing a clear gradient where a lower proportion of lysogenic bacteria resulted in
251 more severe tissue lesions. In a human monocyte (THP-1) infection model used to
252 assess inflammatory response, we found that the non-lysogenic strain significantly
253 increased the production of the pro-inflammatory cytokine IL-6. IL-6 triggers the
254 release of acute-phase response proteins into the bloodstream, leading to a systemic
255 inflammatory response (22). It is also considered a key biomarker for predicting poor
256 outcomes in sepsis patients and is a promising target for inhibitors to help mitigate the
257 adverse effects of inflammation (16, 23). The induction of IL-6 by the non-lysogenic
258 strain may be linked to its heightened virulence and the significant neutrophil
259 recruitment observed at the inflammation site, as evidenced by the histopathological
260 analysis of infected kidneys.

261 The exact trigger causing excision of Φ13 during infection remains to be
262 established. Interestingly, our observations show that after intravenous infection,
263 kidneys of the same mouse can be colonized differently, one kidney by a lysogenic
264 population, while the other harbors a mixed population. This suggests that Φ13
265 excision is likely induced in the kidneys following colonization rather than during the
266 initial spread of bacteria through the bloodstream. Interestingly, a previous study
267 using a rabbit infection model found that bacteria producing β-hemolysin emerged
268 during organ colonization, but this was not observed in the bacterial population
269 recovered from the bloodstream (10). Stress conditions activating the SOS response are
270 known to induce prophage excision. However, despite many attempts, we were not
271 able to induce Φ13 excision from the bacterial chromosome through treatment with
272 Mitomycin C as SOS-inducing agent. Similar results were previously described with a
273 Newman strain carrying the closely related *hlb*-converting prophage, ΦNM3 (24).
274 More recently, it has been demonstrated that exposure to oxidative stress (such as
275 hydrogen peroxide) and biofilm growth conditions promote the excision of ΦSA3mw
276 (25). This may correlate with our in vivo observations, i.e. that phage induction occurs
277 after organ colonization, under biofilm development conditions.

278 Epidemiological studies have shown that *hlb*-converting prophages are more
279 commonly found in strains colonizing humans (from nasal swabs) than in invasive
280 strains (isolated from blood) (3). Additionally, Φ13-derivative carriers are significantly
281 more frequent in human *S. aureus* strains than in animal strains (26). These *hlb*-
282 converting phages not only inactivate *hlb* but also carry virulence genes, including an

283 immune evasion cluster (IEC) (8). The Sak, SCIN, and CHIPS determinants encoded
284 by this cluster play crucial roles in modulating neutrophil chemotaxis, bacterial
285 phagocytosis, and killing (14). However, their activity is highly specific, primarily
286 targeting the human immune system (27-29). This specificity of the Φ13-derivative IEC
287 in counteracting the human immune response likely contributes to the greater
288 prevalence of *hlb*-converting prophages in human *S. aureus* strains.

289 Interestingly, we demonstrated using an infection mouse model, that the *hlb* gene
290 is the major determinant responsible for the increased virulence observed in the
291 absence of the Φ13 phage. When Hlb is produced, no effect of Φ13 alone was observed
292 (Fig. 5B), likely because the strain is already highly virulent due to constant Hlb
293 production. However, in the absence of *hlb*, the presence of Φ13 led to lowered mouse
294 mortality (Fig. 3A and 5A). While the immune evasion factors encoded by Φ13 have
295 been described as human-specific, it cannot be excluded that they may also exhibit
296 some activity during mouse colonization. Alternatively, Φ13 may encode
297 uncharacterized proteins that could modulate *S. aureus* virulence.

298 Excision of Φ13 and the chromosomal rearrangement reconstituting an intact *hlb*
299 gene can be viewed as a timing device, ensuring that the bacteria first colonize the host,
300 benefiting from the immune evasion cluster proteins encoded by the prophage, with
301 production of β-hemolysin and host tissue damage occurring once the bacteria have
302 reached a threshold level, in agreement with the temporal control of *Staphylococcus*
303 *aureus* virulence factors (30). One of the first examples of prophage excision as a timing
304 device for a developmental process is the *skin* element whose excision leads to a
305 chromosomal rearrangement reconstituting the gene encoding the Sigma K sigma
306 factor, essential for *Bacillus subtilis* sporulation (31, 32).

307 As demonstrated in this study and supported by the literature, the
308 heterogeneity within *S. aureus* populations with respect to *hlb*-converting prophages
309 appears to be a common trait. This could be seen as a bet-hedging strategy, allowing
310 the bacteria to retain the ability to produce both immune evasion proteins (in the
311 lysogenic population) and the potent Hlb cytotoxin (in the non-lysogenic cells).
312 Additionally, since both β-hemolysin and the immune evasion cluster proteins
313 encoded by the prophage are secreted, it is plausible that functional complementation
314 may occur within a mixed population of lysogenic and non-lysogenic bacteria. Similar
315 dual strategies have been observed before, where bistability leads to cell-to-cell
316 variation in gene expression (33, 34). This mixed population with distinct genetic

content would be well-equipped both to resist host defenses during colonization and to cause cellular damage.

320 **MATERIALS AND METHODS**

321 **Bacterial strains and growth media**

322

323 *Escherichia coli* K12 strain DH5α™ (Invitrogen) was used for cloning experiments.
324 *Staphylococcus aureus* strain HG001, derived from strain NCTC 8325 by repairing the
325 mutated *rsbU* gene (12), was used for genetic and functional studies. Plasmids were
326 first transformed into the restriction deficient *S. aureus* strain RN4220 before
327 introduction into the HG001 or derivative strains. *E. coli* strains were grown in LB
328 medium with ampicillin (100 μg/mL) added when required. *S. aureus* strains and
329 plasmids used in this study are listed in Supplementary Table 1. *S. aureus* strains were
330 grown in Trypticase Soy Broth (TSB; Difco) supplemented with chloramphenicol (10
331 μg/mL) or erythromycin (1 μg/mL) when required. *E. coli* and *S. aureus* strains were
332 transformed by electroporation using standard protocols (35) and transformants were
333 selected on LB or Trypticase Soy Agar (TSA; Difco) plates, respectively, with the
334 appropriate antibiotics.

335

336 **DNA manipulations**

337

338 Oligonucleotides used in this study were synthesized by Eurofins Genomics and are
339 listed in Supplementary Table 2. *S. aureus* chromosomal DNA was isolated using the
340 MasterPure™ Gram-positive DNA purification Kit (Epicentre Biotechnologies).
341 Plasmid DNA was isolated using a QIAprep Spin Miniprep kit (Qiagen) and PCR
342 fragments were purified using the Qiaquick PCR purification kit (Qiagen). T4 DNA
343 ligase and restriction enzymes, PCR reagents and Q5 high-fidelity DNA polymerase
344 (New England Biolabs) were used according to the manufacturer's recommendations.
345 Nucleotide sequencing of plasmid constructs was carried out by Eurofins Genomics .

346

347 **Plasmids and mutant strain construction**

348

349 Construction of the ΔΦ13 mutant strain was carried out by cloning an 1800 bp DNA
350 fragment centered around the *attB* site, generated by PCR using oligonucleotides
351 OSA418 and OSA419 and chromosomal DNA from the SH1000 strain (a NCTC8325-4
352 derivative cured for prophages), between the *Bam*HI and *Eco*RI sites of the pMAD
353 vector (36), to give plasmid pMAD-Φ13. For deletion of the Φ13 integrase (*int*; *saouhsc-*

354 *02239*), DNA fragments corresponding to the *int* upstream and downstream regions
355 were generated using oligonucleotides OSA411/OSA412 (900 bp) and
356 OSA413/OSA414 (820 bp) cloned between the pMAD *Bam*HI and *Nco*I sites. The *aad*(9)
357 spectinomycin resistance gene (37) was inserted in the center of the 23 nt intergenic
358 region between the convergent Φ13 *saouhsc-02232* and *saouhsc-02233* genes, to avoid
359 any polar effects on transcription. DNA fragments corresponding to the regions
360 upstream and downstream from the insertion site were generated by PCR using
361 primers OSA508/OSA509 and OSA510/OSA511, respectively, and for the *aad*(9)
362 cassette primers OSA299/OSA470 and plasmid pIC333 (38) as the DNA matrix. The
363 DNA fragments were cloned into pMAD using the *Bam*HI/*Sal*I sites for the upstream
364 fragment, *Sal*I/*Nco*I for the *aad*(9) cassette, and the *Nco*I/*Bgl*II sites for the downstream
365 fragment, generating plasmid pMAD-Φ13*aad*(9). For deletion of *hlb*, we generated
366 upstream and downstream fragments by PCR using oligonucleotides
367 OSA442/OSA443 (884 bp) and OSA444/OSA445 (889 bp) respectively. These
368 fragments were introduced into pMAD between the *Bam*HI and *Eco*RI sites, thus
369 generating the pMAD-*hlb* plasmid. To introduce a functional *hlb* allele into the Φ13
370 lysogenic strain, a pMAD-*hlb*comp plasmid was constructed to place the intact *hlb* gene
371 upstream from the Φ13 genome. A PCR fragment including the *hlb* upstream region
372 and the *hlb* intact gene (1760 bp) was generated using the OSA418 and OSA573 primers
373 and the SH1000 genomic DNA as matrix and it was cloned into pMAD using the
374 *BamH*I and *Sal*I restriction sites. A second PCR fragment corresponding to the part of
375 Φ13 adjacent to *att*L was generated with the OSA574-575 primers and cloned between
376 the *Sal*I and *Bgl*II restriction sites of pMAD.
377 Plasmids were introduced by electroporation into *S. aureus* strain RN4220, and
378 transformants selected at 30°C on TSA plates containing erythromycin and 5-bromo-
379 4-chloro-3-indolyl-β-D-galactopyranoside (X-Gal) (100 μg/mL). Plasmids were then
380 introduced into strain HG001 and integration and excision performed as previously
381 described (36), yielding strains HG001ΔΦ13, HG001Δ*int*, and HG001Φ13-aad(9) and
382 into strain HG001ΔΦ13 for pMAD-*hlb* and HG001Δ*int* for pMAD-*hlb*comp to give
383 strains HG001Δ*int hlb*comp, HG001ΔΦ13Δ*hlb*.
384 Plasmid pMK4Pprot-*int* was used for complementation of the Δ*int* mutant and
385 constructed by cloning the entire *int* coding sequence (amplicon OSA446/OSA447)
386 under the control of the constitutive P*prot* promoter (39).
387

388 **Prophage content measurement by quantitative real time PCRs (qRT-PCRs)**

389

390 Strains were grown overnight in TSB at 37°C, with aeration. Cells were pelleted by
391 centrifugation (2 min, 20,800 *g*) from 2 mL culture samples and genomic DNA
392 extracted using the MasterPure™ Gram Positive DNA Purification Kit (Tebu-Bio).
393 Oligonucleotides were designed with the BEACON Designer 4.02 software
394 (Premier Biosoft International, Palo Alto, CA) to synthesize 100-200 bp amplicons (see
395 Supplementary Table 2). Quantitative real-time PCRs (qRT-PCRs) and critical
396 threshold cycles (CT) were performed and determined using the SsoFast™ EvaGreen
397 Supermix (Bio-Rad, Hercules, CA). All assays were performed using quadruplicate
398 technical replicates, and repeated with three independent biological samples, with one
399 representative experiment shown. Prophage loss frequency was calculated using the
400 formula: $1/(1+2^{\Delta Ct})$ derived from the ΔCt method (40).

401

402 **Hemolysis detection**

403

404 Bacteria were grown overnight in TSB at 37°C with aeration. Culture aliquots (3 µl)
405 were spotted on Columbia plates containing 5% sheep blood (COS, Biomerieux
406 Craponne). Plates were incubated for 24h at 37°C and transferred to 4°C for an
407 additional 24h to for detection of β-hemolysis (41).

408

409 **THP-1 infection experiments**

410

411 THP-1 monocytes were maintained as previously described (42). Differentiation and
412 adherence were obtained by incubation with Phorbol 12-Myristate 13-Acetate (PMA,
413 50 ng/mL) during 4 days at 37°C in a 5%CO_2 atmosphere. Bacterial uptake
414 experiments and survival assays were carried out as previously described (43). Briefly,
415 bacteria were grown in TSB until OD_{600nm} = 1. Cultures were washed in PBS and
416 adjusted to the desired inoculum in RPMI 1640 medium (Gibco), and c.f.u. counts
417 determined by plating serial dilutions on TSA plates. Differentiated THP-1
418 macrophages were incubated with bacteria (MOI = 10) in RPMI 1640 at 37°C with 5%
419 CO2 for 1 h to allow bacterial phagocytosis. They were then washed with RPMI and
420 incubated in RPMI-10% Fetal Calf Serum with streptomycin (100 µg/mL), penicillin
421 (100 U/mL), and gentamycin 40 µg/mL to eliminate extracellular bacteria. At the

422 indicated times, infected macrophages were washed once with RPMI and lysed by
423 incubation in ice-cold water for 15 min and c.f.u. counts were determined by plating
424 serial dilutions on TSA plates. For cytokine gene expression studies by qRT-PCR, THP-
425 1 cells were frozen at -20°C 24h post-infection. Total RNA was extracted using a
426 RNeasy mini kit (Qiagen, CA, USA). Cytokine gene expression was analysed by qRT-
427 PCR using the StepOnePlus real-time PCR system (Applied Biosystems). Primers used
428 for qRT-PCR were TNFα, IL6, pro-IL1beta and HPRT as the reference gene. The qRT-
429 PCRs were performed by Taqman and results presented as relative quantification of
430 gene expression using the $2^{-\Delta\Delta CT}$ method.
431
432 **Animal experiments**
433
434 Seven-week-old female *RjOrl:SWISS* mice (Janvier Labs) were inoculated
435 intravenously with the specified *S. aureus* strains. To analyse Φ13 excision during the
436 infectious process, mice were infected with a sublethal dose (2 x 10^7 c.f.u.) of the Φ13-
437 *aad*(9) strain. Mice were sacrificed four days post-infection and kidneys harvested and
438 homogenized for c.f.u. determination following dilution and plating on TSA and TSA
439 with spectinomycin (100 µg/mL). The rate of prophage excision was calculated as
440 [(c.f.u. on TSA) - (c.f.u. on TSA+spectinomycin)]/(c.f.u. on TSA).
441 Strain HG001 and the Δ*int*, ΔΦ*13*, ΔΦ*13*Δ*hlb* and Δ*int hlb*comp mutants were used
442 for survival studies. Groups of seven mice were injected in the caudal lateral vein with
443 5 X 10^7 c.f.u. per mouse in 0.2 mL. Survival was monitored daily for 9 days following
444 infection and three independent experiments were carried out. To measure kidney
445 colonization and histopathological analysis, mice were infected intravenously with a
446 sublethal dose (1 X 10^7 c.f.u.) of the HG001 parental and Δ*int* and ΔΦ*13* mutant strains
447 (six mice for each strain). At six days post-infection, kidneys were collected and for
448 each mouse, bacterial c.f.u. counts were carried out using one kidney and
449 histopathological observations were done on the other kidney. For histopathology,
450 kidneys were removed and immediately fixed in 10% neutral buffered formalin. After
451 48 h of fixation, the kidneys were longitudinally sectioned through the hilus in order
452 to obtain the renal cortex, medulla, crest, and pelvis on the same section. These
453 samples were embedded in paraffin, and 4-µm sections were cut and stained with
454 hematoxylin and eosin (lesion description) and Gram (bacterial detection).
455

Ethics statement

Animal experiments were carried out at the Institut Pasteur according to European Union guidelines for handling of laboratory animals (http://ec.europa.eu/environment/chemicals/lab_animals/index_en.htm). Animals were monitored daily with a particular attention for any signs of distress. Protocols used were approved by the Institut Pasteur ethics committee (dap160057).

ACKNOWLEDGMENTS

We are grateful to Patrick Trieu-Cuot, in whose lab this work was carried out, and Shaynoor Dramsi for helpful discussion. All authors have read and agreed to the submitted version of the manuscript.

FUNDING

This work was supported by funds from Institut Pasteur, CNRS, and Vaincre La Mucoviscidose Association (Grant «Phage induction, a novel essential factor for *Staphylococcus aureus* infections?»).

AUTHOR CONTRIBUTIONS

Conceptualization: Sarah Dubrac, Lhousseine Touqui, Tarek Msadek.
Data curation: Olivier Poupel, Sarah Dubrac, Lhousseine Touqui, Tarek Msadek.
Formal analysis: Sarah Dubrac, Grégory Jouvion, Lhousseine Touqui, Tarek Msadek.
Funding acquisition: Sarah Dubrac, Lhousseine Touqui, Tarek Msadek.
Investigation: Olivier Poupel, Gérard Kénanian, Charlotte Abrial, Sarah Dubrac.
Methodology: Olivier Poupel, Sarah Dubrac.
Project administration: Tarek Msadek, Sarah Dubrac.
Resources: Tarek Msadek, Sarah Dubrac.
Supervision: Tarek Msadek, Sarah Dubrac.
Validation: Tarek Msadek, Sarah Dubrac.
Writing – original draft: Tarek Msadek, Sarah Dubrac.
Writing – review & editing: Tarek Msadek, Sarah Dubrac.

ADDITIONAL FILES

The following material is available online.

Supplemental Material

Supplemental Figures and Tables. Fig. S1–S4 and Tables S1–S2.

499 **REFERENCES**
500

501 1. Piewngam P, Otto M. 2024. *Staphylococcus aureus* colonisation and strategies for
502 decolonisation. Lancet Microbe 5:e606-e618.
503 2. Fitzgerald JR, Sturdevant DE, Mackie SM, Gill SR, Musser JM. 2001.
504 Evolutionary genomics of *Staphylococcus aureus*: insights into the origin of
505 methicillin-resistant strains and the toxic shock syndrome epidemic. Proc. Nat.
506 Acad. Sci. USA: 98:8821-6.
507 3. Goerke C, Pantucek R, Holtfreter S, Schulte B, Zink M, Grumann D, Broker BM,
508 Doskar J, Wolz C. 2009. Diversity of prophages in dominant *Staphylococcus*
509 *aureus* clonal lineages. J. Bacteriol. 191:3462-8.
510 4. Xia G, Wolz C. 2014. Phages of *Staphylococcus aureus* and their impact on host
511 evolution. Infect. Genet. Evol. 21:593-601.
512 5. Goerke C, Wirtz C, Fluckiger U, Wolz C. 2006. Extensive phage dynamics in
513 *Staphylococcus aureus* contributes to adaptation to the human host during
514 infection. Mol. Microbiol.61:1673-85.
515 6. Feiner R, Argov T, Rabinovich L, Sigal N, Borovok I, Herskovits AA. 2015. A
516 new perspective on lysogeny: prophages as active regulatory switches of
517 bacteria. Nat. Rev. Microbiol. 13:641-50.
518 7. Iandolo JJ, Worrell V, Groicher KH, Qian Y, Tian R, Kenton S, Dorman A, Ji H,
519 Lin S, Loh P, Qi S, Zhu H, Roe BA. 2002. Comparative analysis of the genomes
520 of the temperate bacteriophages phi 11, phi 12 and phi 13 of *Staphylococcus*
521 *aureus* 8325. Gene 289:109-18.
522 8. van Wamel WJ, Rooijakkers SH, Ruyken M, van Kessel KP, van Strijp JA. 2006.
523 The innate immune modulators staphylococcal complement inhibitor and
524 chemotaxis inhibitory protein of *Staphylococcus aureus* are located on beta-
525 hemolysin-converting bacteriophages. J. Bacteriol. 188:1310-5.
526 9. Rohmer C, Wolz C. 2021. The role of hlb-converting bacteriophages in
527 *Staphylococcus aureus* host adaption. Microb. Physiol. 31:109-122.
528 10. Salgado-Pabon W, Herrera A, Vu BG, Stach CS, Merriman JA, Spaulding AR,
529 Schlievert PM. 2014. *Staphylococcus aureus* beta-toxin production is common in
530 strains with the beta-toxin gene inactivated by bacteriophage. J. Infect. Dis.
531 146:784-92.
532 11. Katayama Y, Baba T, Sekine M, Fukuda M, Hiramatsu K. 2013. Beta-hemolysin
533 promotes skin colonization by *Staphylococcus aureus*. Journal of Bacteriology
534 195:1194-203.

535 12. Herbert S, Ziebandt AK, Ohlsen K, Schafer T, Hecker M, Albrecht D, Novick R,
536 Gotz F. 2010. Repair of global regulators in *Staphylococcus aureus* 8325 and
537 comparative analysis with other clinical isolates. Infect. Immun. 78:2877-89.
538 13. Gillaspy AF, Worrell V, Orvis J, Roe BA, Dyer DW, Iandolo JJ. 2006. The
539 *Staphylococcus aureus* NCTC 8325 Genome, p 381-412. *In* Fischetti VA, Novick
540 RP, Ferretti JJ, Portnoy DA, Rood JI (ed), Gram-Positive Pathogens, 2nd ed.
541 ASM Press, Washington, DC.
542 14. Rooijakkers SH, van Kessel KP, van Strijp JA. 2005. Staphylococcal innate
543 immune evasion. Trends Microbiol. 13:596-601.
544 15. Nunes-Duby SE, Kwon HJ, Tirumalai RS, Ellenberger T, Landy A. 1998.
545 Similarities and differences among 105 members of the Int family of site-specific
546 recombinases. Nucleic Acids Res. 26:391-406.
547 16. van den Berg S, Laman JD, Boon L, ten Kate MT, de Knegt GJ, Verdijk RM,
548 Verbrugh HA, Nouwen JL, Bakker-Woudenberg IA. 2013. Distinctive cytokines
549 as biomarkers predicting fatal outcome of severe *Staphylococcus aureus*
550 bacteremia in mice. PLoS One 8:e59107.
551 17. Haag AF, Bagnoli F. 2017. The role of two-component signal transduction
552 systems in *Staphylococcus aureus* virulence regulation. Curr. Top. Microbiol.
553 Immunol. 409:145-198.
554 18. Lindsay JA. 2010. Genomic variation and evolution of *Staphylococcus aureus*. Int
555 J. Med. Microbiol. 300:98-103.
556 19. Huseby M, Shi K, Brown CK, Digre J, Mengistu F, Seo KS, Bohach GA,
557 Schlievert PM, Ohlendorf DH, Earhart CA. 2007. Structure and biological
558 activities of beta toxin from *Staphylococcus aureus*. J. Bacteriol. 189:8719-26.
559 20. Herrera A, Vu BG, Stach CS, Merriman JA, Horswill AR, Salgado-Pabon W,
560 Schlievert PM. 2016. *Staphylococcus aureus* beta-toxin mutants are defective in
561 biofilm ligase and sphingomyelinase activity, and causation of infective
562 endocarditis and sepsis. Biochemistry 55:2510-7.
563 21. Huseby MJ, Kruse AC, Digre J, Kohler PL, Vocke JA, Mann EE, Bayles KW,
564 Bohach GA, Schlievert PM, Ohlendorf DH, Earhart CA. 2010. Beta toxin
565 catalyzes formation of nucleoprotein matrix in staphylococcal biofilms. Proc.
566 Nat. Acad. Sci. USA: 107:14407-12.
567 22. Tanaka T, Narazaki M, Kishimoto T. 2014. IL-6 in inflammation, immunity, and
568 disease. Cold Spring Harb. Perspect. Biol. 6:a016295.

569 23. Cao YZ, Tu YY, Chen X, Wang BL, Zhong YX, Liu MH. 2012. Protective effect
570 of Ulinastatin against murine models of sepsis: inhibition of TNF-alpha and IL-
571 6 and augmentation of IL-10 and IL-13. Exp. Toxicol. Pathol. 64:543-7.
572 24. Bae T, Baba T, Hiramatsu K, Schneewind O. 2006. Prophages of *Staphylococcus*
573 *aureus* Newman and their contribution to virulence. Mol. Microbiol. 62:1035-47.
574 25. Tran PM, Feiss M, Kinney KJ, Salgado-Pabon W. 2019. ØSa3mw prophage as a
575 molecular regulatory switch of *Staphylococcus aureus* β-toxin production. J.
576 Bacteriol. 201:e00766-18
577 26. Verkaik NJ, Benard M, Boelens HA, de Vogel CP, Nouwen JL, Verbrugh HA,
578 Melles DC, van Belkum A, van Wamel WJ. 2011. Immune evasion cluster-
579 positive bacteriophages are highly prevalent among human *Staphylococcus*
580 *aureus* strains, but they are not essential in the first stages of nasal colonization.
581 Clin. Microbiol. Infect. 17:343-8.
582 27. de Haas CJ, Veldkamp KE, Peschel A, Weerkamp F, Van Wamel WJ, Heezius
583 EC, Poppelier MJ, Van Kessel KP, van Strijp JA. 2004. Chemotaxis inhibitory
584 protein of *Staphylococcus aureus*, a bacterial antiinflammatory agent. J. Exp. Med.
585 199:687-95.
586 28. Kwiecinski J, Josefsson E, Mitchell J, Higgins J, Magnusson M, Foster T, Jin T,
587 Bokarewa M. 2010. Activation of plasminogen by staphylokinase reduces the
588 severity of *Staphylococcus aureus* systemic infection. J. Infect. Dis. 202:1041-9.
589 29. Rooijakkers SH, Ruyken M, Roos A, Daha MR, Presanis JS, Sim RB, van Wamel
590 WJ, van Kessel KP, van Strijp JA. 2005. Immune evasion by a staphylococcal
591 complement inhibitor that acts on C3 convertases. Nat. Immunol. 6:920-7.
592 30. Novick RP. 2003. Autoinduction and signal transduction in the regulation of
593 staphylococcal virulence. Mol. Microbiol. 48:1429-49.
594 31. Stragier P, Kunkel B, Kroos L, Losick R. 1989. Chromosomal rearrangement
595 generating a composite gene for a developmental transcription factor. Science
596 243:507-12.
597 32. Kunkel B, Losick R, Stragier P. 1990. The *Bacillus subtilis* gene for the
598 development transcription factor sigma K is generated by excision of a
599 dispensable DNA element containing a sporulation recombinase gene. Genes
600 Dev. 4:525-35.
601 33. Dubnau D, Losick R. 2006. Bistability in bacteria. Mol. Microbiol. 61:564-72.
602 34. Veening JW, Smits WK, Kuipers OP. 2008. Bistability, epigenetics, and bet-
603 hedging in bacteria. Annu. Rev. Microbiol. 62:193-210.

604 35. Sambrook J, Fritsch EF, Maniatis T. 1989. Molecular cloning : a laboratory
605 manual, second edition. Cold Spring Harbor Laboratory, Cold Spring Harbor,
606 N. Y.
607 36. Arnaud M, Chastanet A, Debarbouille M. 2004. New vector for efficient allelic
608 replacement in naturally nontransformable, low-GC-content, gram-positive
609 bacteria. Appl. Environ. Microbiol. 70:6887-91.
610 37. Murphy E. 1985. Nucleotide sequence of a spectinomycin adenyltransferase
611 AAD(9) determinant from *Staphylococcus aureus* and its relationship to AAD(3")
612 (9). Mol. Gen. Genet. 200:33-39.
613 38. Steinmetz M, Richter R. 1994. Easy cloning of mini-Tn*10* insertions from the
614 *Bacillus subtilis* chromosome. J. Bacteriol. 176:1761-3.
615 39. Archambaud C, Gouin E, Pizarro-Cerda J, Cossart P, Dussurget O. 2005.
616 Translation elongation factor EF-Tu is a target for Stp, a serine-threonine
617 phosphatase involved in virulence of *Listeria monocytogenes*. Mol. Microbiol.
618 56:383-96.
619 40. Livak KJ, Schmittgen TD. 2001. Analysis of relative gene expression data using
620 real-time quantitative PCR and the 2(-Delta Delta C(T)) method. Methods
621 25:402-8.
622 41. Haque RU, Baldwin JN. 1964. Types of hemolysins produced by *Staphylococcus*
623 *aureus*, as determined by the replica plating technique. J. Bacteriol. 88:1442-7.
624 42. Stokes RW, Doxsee D. 1999. The receptor-mediated uptake, survival, replication,
625 and drug sensitivity of *Mycobacterium tuberculosis* within the macrophage-like
626 cell line THP-1: a comparison with human monocyte-derived macrophages.
627 Cell. Immunol. 197:1-9.
628 43. Soutourina O, Dubrac S, Poupel O, Msadek T, Martin-Verstraete I. 2010. The
629 pleiotropic CymR regulator of *Staphylococcus aureus* plays an important role in
630 virulence and stress response. PLoS Pathog. 6:e1000894.
631

632 **FIGURE LEGENDS**
633
634 **Figure 1: Prophage Φ13 in vitro and in vivo.** A) Prophage excision frequencies in
635 strain HG001. qRT-PCR quantification of Φ11, 12, and 13 prophage content in *S. aureus*
636 strain HG001 grown in TSB at 37°C with aeration. Specific primer pairs are described
637 in Supplementary Table 3. The results are the mean of 4 technical replicates and are
638 representative of 3 independent biological replicates.
639 B) Quantification of Φ13 lysogens in bacterial populations from infected kidneys. Mice
640 were infected from the caudal lateral vein with a sub-lethal dose (2 X 10^7 c.f.u.) of *S.*
641 *aureus* strain HG001 Φ13::*aad*(9). Mice were sacrificed four days post-infection and
642 kidneys harvested for c.f.u. counts on TSA and TSA with spectinomycin. 25 infected
643 kidneys were examined and the proportion of homogeneous lysogen population (less
644 than 0.5% non-lysogen) and heterogeneous bacterial population with a mix of lysogen
645 and non-lysogen bacteria is shown.
646 C) Proportion of non-lysogen bacteria per kidney in organs infected with a mixed
647 population of lysogenic and non-lysogenic bacteria.
648
649 **Figure 2: Characterization of the *S. aureus* Δ*int* and ΔΦ13 mutants.** Strains were
650 grown overnight at 37°C with aeration. A) 3 µl of the bacterial cultures was spotted on
651 sheep blood agar plates and incubated consecutively for 24 h at 37°C and 24 h at 4°C
652 to detect hemolytic activities. The white arrow indicates the β-hemolytic halo
653 characteristic of bacteria lacking prophage Φ13. B) Prophage Φ13 excision frequency
654 detected by qRT-PCR using oligonucleotide pairs OMA7-OMA8 and OMA7-OMA9
655 specific for the presence or absence of Φ13, respectively.
656
657 **Figure 3: Impact of prophage Φ13 and *hlb* on *S. aureus* virulence.** A) Kaplan-Meier
658 survival curves of *RjOrl:SWISS* mice infected intravenously with *S. aureus* HG001 wild
659 type strain and the Δ*int* and ΔΦ13 mutants (5 X 10^7 c.f.u./injection). A total of 14 mice
660 were used in each group in two independent experiments. *, $P<0.05$ and **, $P<0.01$
661 (Wilcoxon test). For each strain, the genotype is indicated followed by the relevant
662 genetic context (presence or absence of prophage Φ13 and a functional *hlb* gene). B)
663 Histopathological kidney analyses 6 days post-infection by intravenous inoculation
664 with sub-lethal bacterial loads (2 X 10^7 c.f.u./injection) of the *S. aureus* HG001 wild

665 type (1 and 2), Δ*int* (3 and 4) and ΔΦ13 (5 and 6) strains. Most (5/6) mice infected with
666 the wild type strain displayed mild to moderate nephritis, with neutrophilic
667 infiltrates/abscesses (black arrowheads) of varying sizes in the cortex (1), medulla, and
668 papilla (2). Infection with strain ΔΦ13 led to more severe nephritis (5/6 mice), with
669 multifocal abscesses (3 and 4, black arrowheads), extension to tubules and interstitium,
670 and ischemic necrosis of the papilla (4, black arrow). Most mice (4/6) infected with the
671 Δ*int* strain displayed less severe lesions, with mononuclear cell infiltrates most often
672 in the cortex (5, not seen at a low magnification) but also in the papilla (6, arrowhead).
673

674 **Figure 4: Impact of Φ13 on cytokine induction by THP-1 neutrophils.** PMA-activated
675 THP-1 cells were infected with the HG001 wild type strain or the ΔΦ13 and Δ*int*
676 mutants with a MOI=10. After 24 H of infection, cytokine gene expression was
677 determined by qRT-PCR performed with cDNA synthesized from RNA of THP-1 cells
678 infected by the indicated strains (dark grey) or non-infected control (light grey).
679 Expression levels are given in arbitrary units normalized against that of HPRT. Each
680 experiment was carried out 6 times in two independent series (means +/- SD). ***:
681 $P<0.005$ (Student's *t*-test).
682

683 **Figure 5: Impact of *hlb* on *S. aureus* virulence.** Kaplan-Meier survival curves of
684 *RjOrl:SWISS* mice infected intravenously with *S. aureus* HG001 wild type strain and
685 the Δ*int* hlb_{comp}, ΔΦ13 and ΔΦ13Δ*hlb* mutants (5×10^7 c.f.u./injection). A total of 14 mice
686 were used in each group in two independent experiments. *, $P<0.05$ and **, $P<0.01$
687 (Wilcoxon test). For each strain, the genotype is indicated followed by the relevant
688 genetic context (presence or absence of prophage Φ13 and a functional *hlb* gene).
689 A) Role of *hlb* in virulence by comparing infection with the HG001 strain and the ΔΦ13
690 and ΔΦ13Δ*hlb* derivatives.
691 B) Role of Φ13 in virulence by comparing infection with the HG001 strain and the
692 Δ*int* hlb_{comp} (dashed line) and ΔΦ13 derivatives.

Figure 1

A.

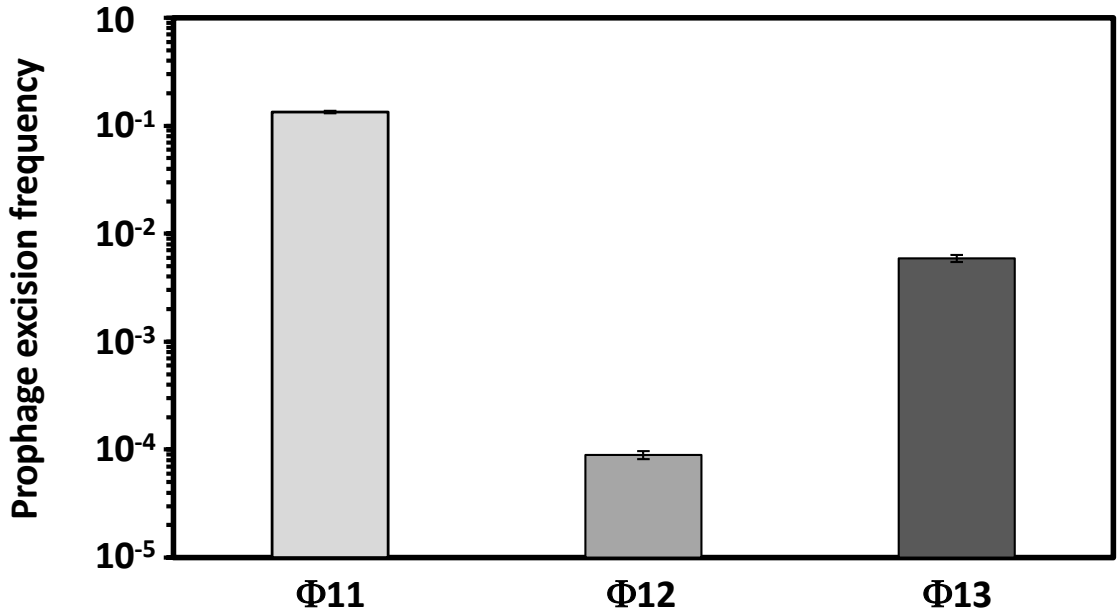
Prophage excision frequency
10
10-1
10-2
10-3
10-4
10-5
Φ11
Φ12
Φ13

B.

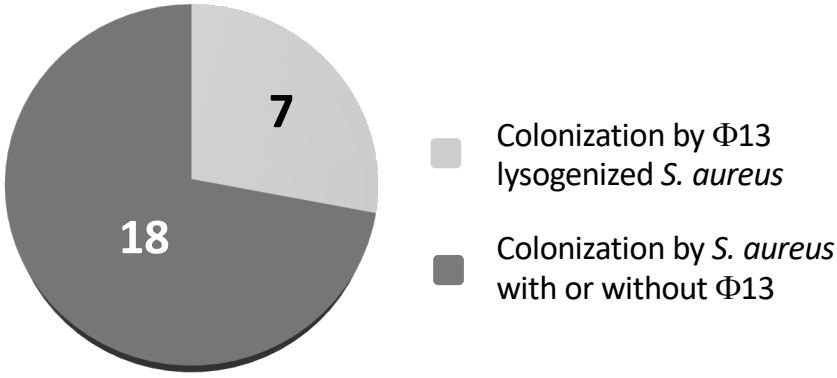
7
18
Colonization by Φ13 lysogenized *S. aureus*
Colonization by *S. aureus* with or without Φ13

C.

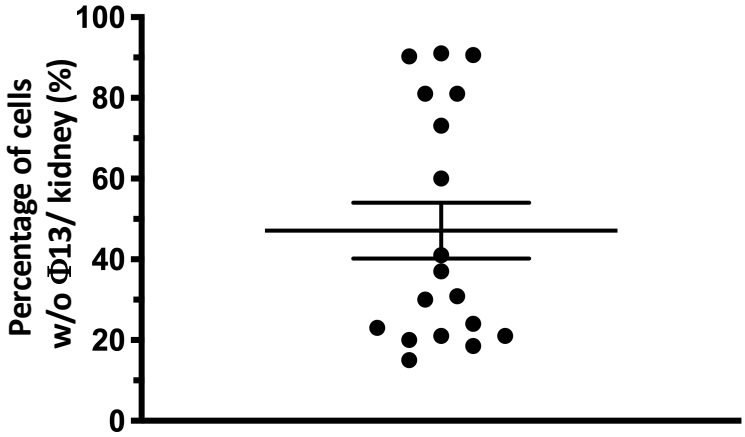
Percentage of cells w/o Φ13/ kidney (%)
100
80
60
40
20
0

Figure 2

A.

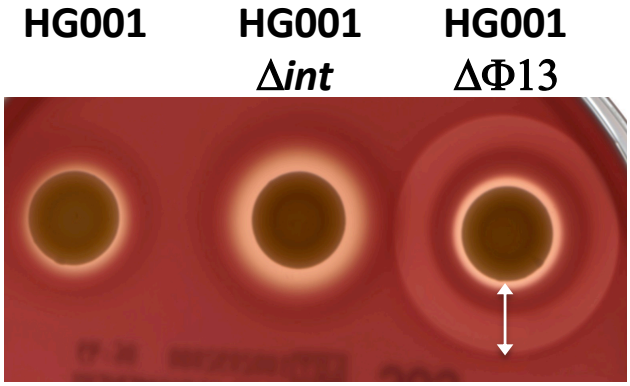
HG001
HG001
Δint
HG001
ΔΦ13

B.

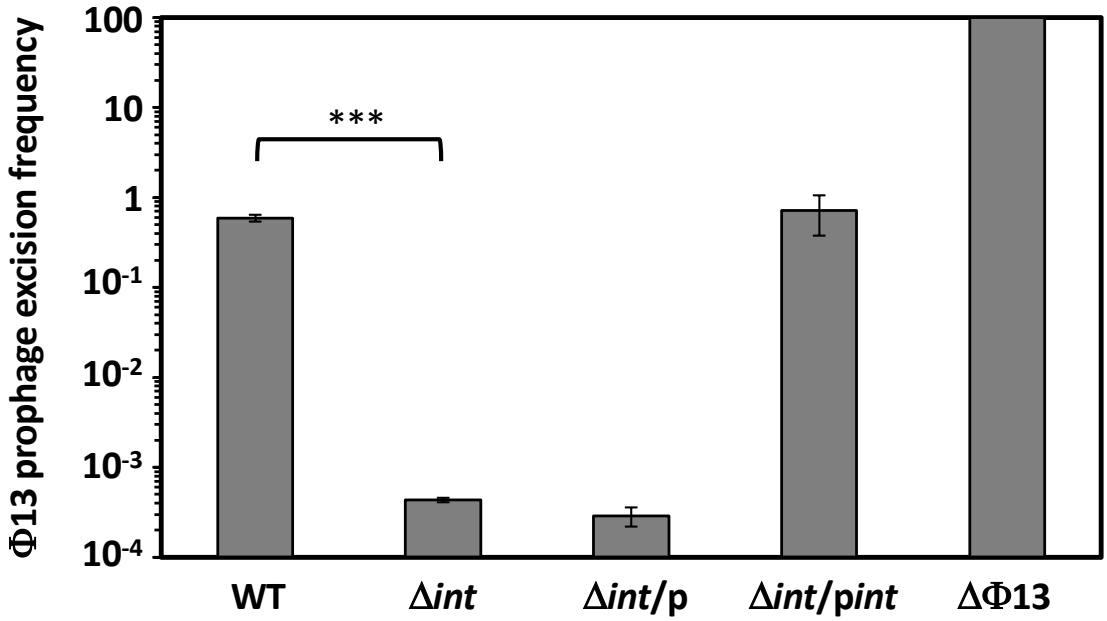
Φ13 prophage excision frequency
100
10
1
10-1
10-2
10-3
10-4
***
WT
Δint
Δint/p
Δint/pint
ΔΦ13

Figure 3

A.

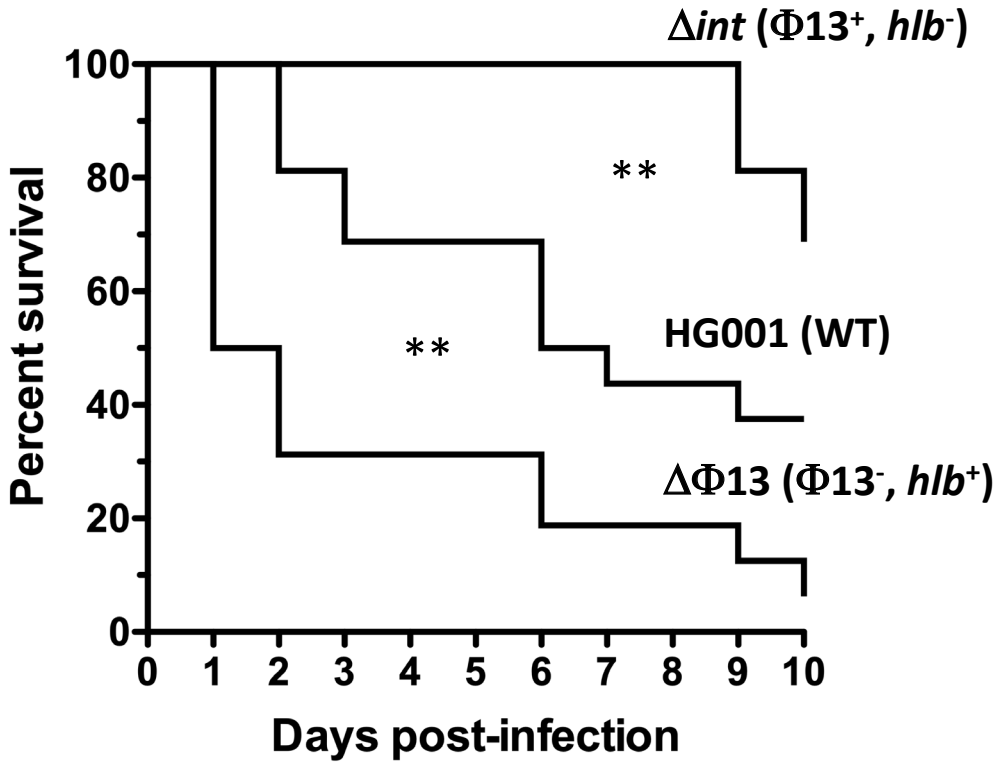
Δint (Φ13+, hlb-)
HG001 (WT)
ΔΦ13 (Φ13-, hlb+)
**
**
Percent survival
100
80
60
40
20
0
0 1 2 3 4 5 6 7 8 9 10
Days post-infection

B.

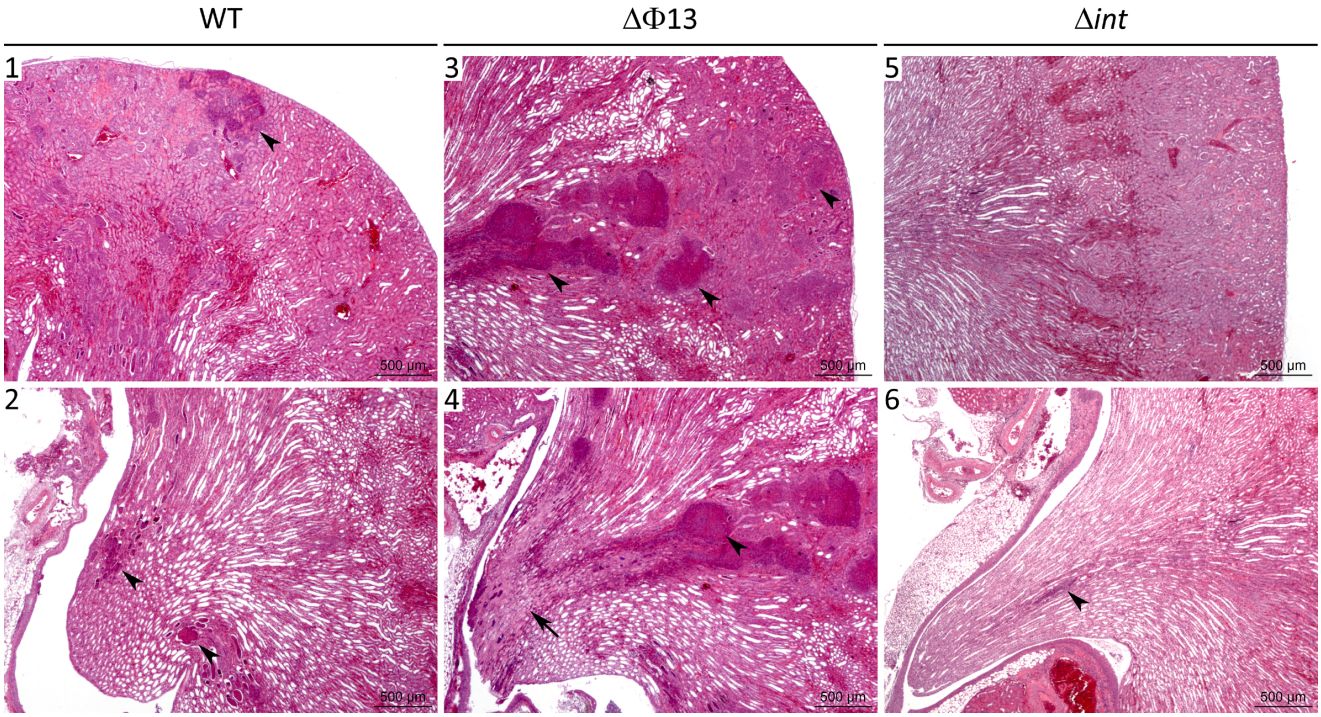
WT
ΔΦ13
Δint
1
2
3
4
5
6
500 µm

Figure 4

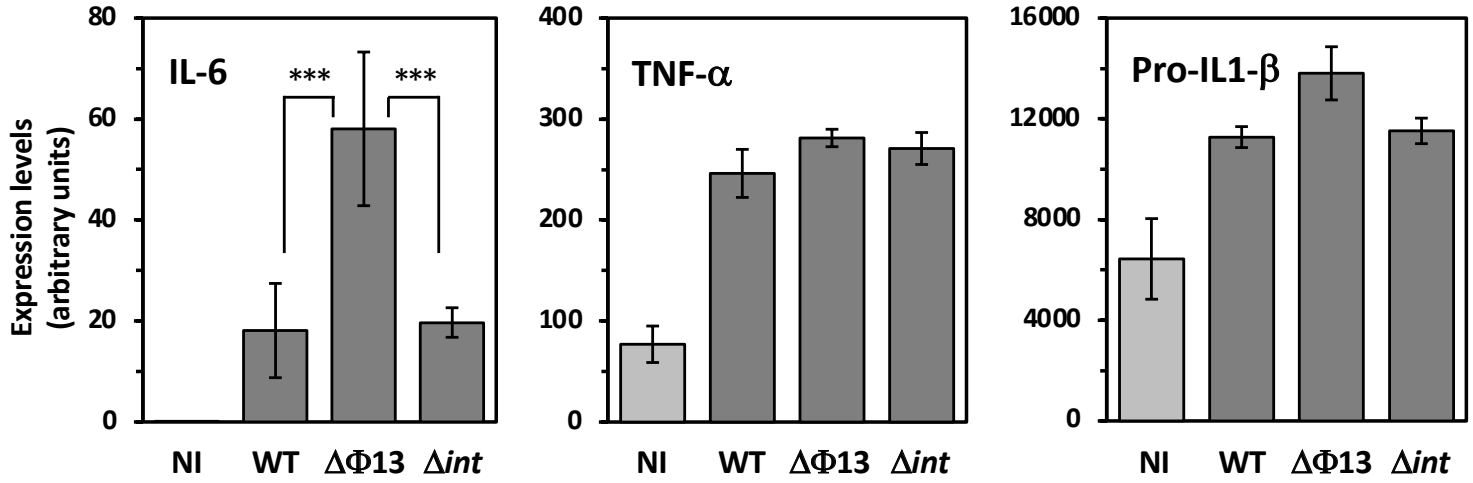
Expression levels (arbitrary units)
IL-6
***
***
80
60
40
20
0
NI
WT
ΔΦ13
Δint
TNF-α
400
300
200
100
0
NI
WT
ΔΦ13
Δint
Pro-IL1-β
16000
12000
8000
4000
0
NI
WT
ΔΦ13
Δint

Figure 5

A.

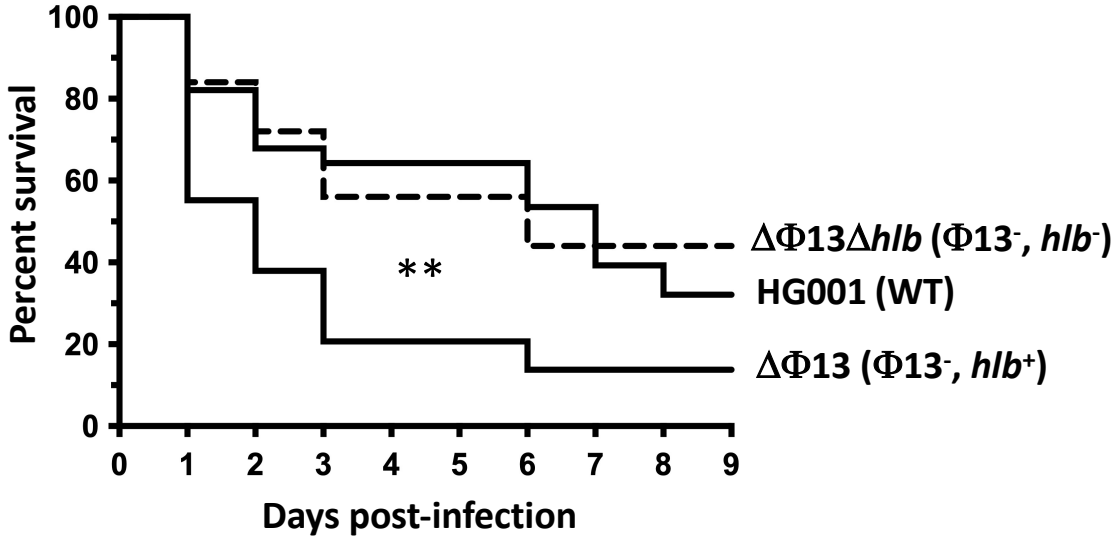
100
80
60
40
20
0
Percent survival
0 1 2 3 4 5 6 7 8 9
Days post-infection
**
ΔΦ13Δhlb (Φ13-, hlb-)
HG001 (WT)
ΔΦ13 (Φ13-, hlb+)

B.

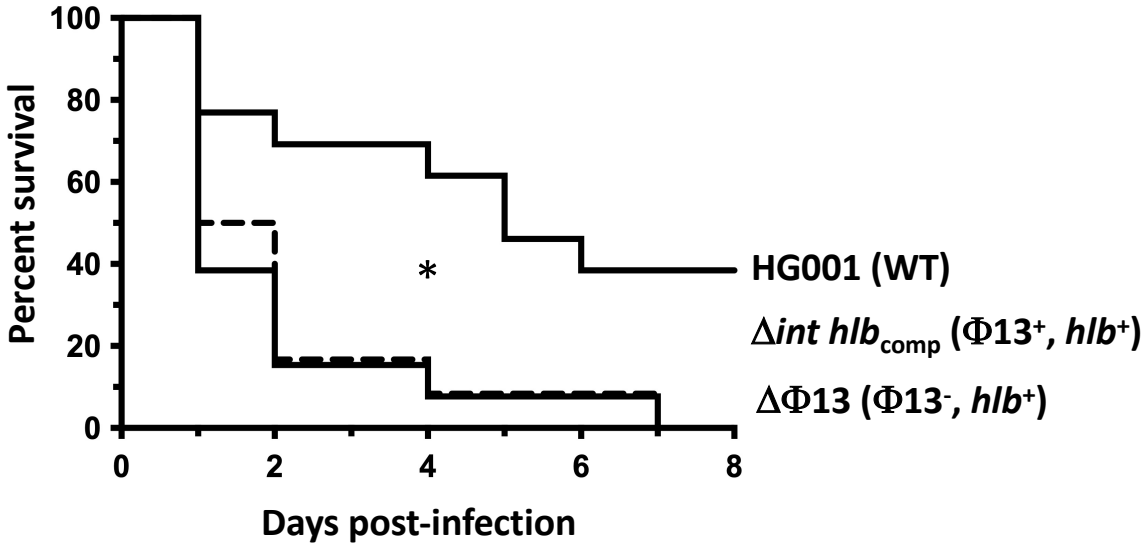
100
80
60
40
20
0
Percent survival
0 2 4 6 8
Days post-infection
*
HG001 (WT)
Δint hlbcomp (Φ13+, hlb+)
ΔΦ13 (Φ13-, hlb+)